A state-of-the-art review on rolling resistance of asphalt pavements and its environmental impact

Sun, Zhaojie; Premarathna, W. A.A.S.; Anupam, Kumar; Kasbergen, Cor; M.J.G. Erkens, Sandra

DOI
10.1016/j.conbuildmat.2023.133589

Publication date
2023

Document Version
Final published version

Published in
Construction and Building Materials

Construction and Building Materials 411 (2024) 133589

Contents lists available at ScienceDirect

Construction and Building Materials

journal homepage: www.elsevier.com/locate/conbuildmat

Review

A state-of-the-art review on rolling resistance of asphalt pavements and its environmental impact

Zhaojie Sun, W.A.A.S. Premarathna, Kumar Anupam *, Cor Kasbergen, Sandra M.J.G. Erkens

Section of Pavement Engineering, Faculty of Civil Engineering and Geosciences, Delft University of Technology, Stevinweg 1, 2628 CN, Delft, The Netherlands

ARTICLE INFO

Keywords:
Asphalt pavement
Rolling resistance
Surface texture
Fuel consumption
Environmental impact

ABSTRACT

In the context of climate change and global warming, the attention on the environmental cost of pavements is increasing. To scientifically quantify the environmental cost of pavements, accurate prediction of rolling resistance and fuel consumption is important. In this paper, a comprehensive review on rolling resistance of asphalt pavements and its environmental impact was presented. At first, the commonly used definitions of rolling resistance and texture characterisation methods of pavement surface were introduced. Then, the influence of different factors on rolling resistance was discussed. Next, the measuring and modelling approaches of rolling resistance were reviewed. At last, methods which can be used to predict fuel consumption and environmental impact were presented. It was found that an ideal approach for texture characterisation of pavement surface is to make use of the entire wavelength spectrum of road profiles and consider the enveloping curve of tire treads. Furthermore, the fact that rolling resistance can be influenced by different factors introduces difficulties in accurate measurement and modelling of rolling resistance. Moreover, testing methods and conditions have a significant effect on the empirical modelling of rolling resistance, while it is difficult and time-consuming to consider all the energy loss in the computational modelling of rolling resistance. In addition, the prediction of fuel consumption and environmental impact highly depends on the formulating methods and measuring conditions. The work presented in this paper will help to gain more insight into rolling resistance and its environmental impact, which ultimately promotes the construction of environmentally friendly pavements.

1. Introduction

The expansion of global transportation networks is damaging the environment because of the endless emission of Greenhouse Gases (GHGs) caused by the consumption of fossil fuels, especially the release of carbon dioxide [1–3]. In order to maintain the environmental health and promote the sustainable development of society, the reduction of carbon emissions has been a goal of many countries in recent years [4,5]. In this direction, the Paris agreement and the Kyoto protocol were formulated to make the reduction of carbon emissions to be a goal of global initiatives [4–6]. Hence, policymakers, researchers, and contractors are continuously making efforts to quantify and control carbon emissions by introducing new policies and optimising existing systems. A significant amount of carbon emissions come from the transportation sector, so it is a moral obligation for transportation community to reduce the carbon footprint [7]. To solve this growing problem, transportation policy makers, researchers, asset managers, and contractors have to gather together.

Several scientific reports [8–10] have indicated that the transportation sector bears about 37 % of the global carbon dioxide emissions, which is the second largest contributor that is only slightly lower than the electricity and heat sector (41 %). Moreover, it was also reported that the transportation sector accounted for 8.22 Gt of annual carbon emissions at the end of the year 2019 [10]. Recently, a scientific report [8] estimated that about 5.86 Gt of global carbon dioxide emission was related to the pavement-based transportation sub-sector. It was significantly higher than the sub-sectors of rail (0.09 Gt), shipping (0.84 Gt), and aviation (0.71 Gt). Furthermore, according to the European Union (EU) transport report in the year 2022 [11], the pavement transportation sub-sector has accounted for about 77 % of carbon emissions all over the 27 EU countries. Based on the aforementioned factors, it can be concluded that global warming and ecosystem stability are more vulnerable to pavement-oriented conveyances [12].

Typically, pavement-based conveyances experience notable energy

* Corresponding author at: Section of Pavement Engineering, Faculty of Civil Engineering and Geosciences, Delft University of Technology, Stevinweg 1, 2628 CN, Delft, The Netherlands.

E-mail address: k.anupam@tudelft.nl (K. Anupam).

https://doi.org/10.1016/j.conbuildmat.2023.133589
Received 5 July 2023; Received in revised form 25 September 2023; Accepted 28 September 2023
Available online 4 December 2023
0950-0618/

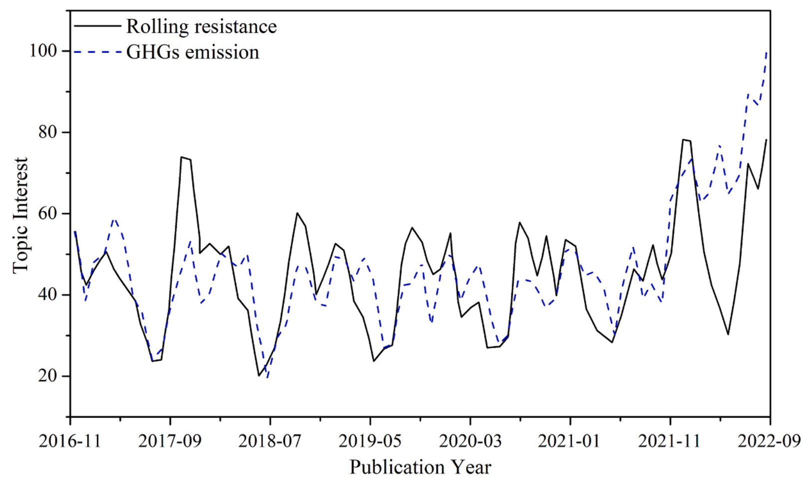

Fig. 1. Topic interest in rolling resistance and GHG emissions based on year [33].

loss due to the aerodynamic drag, gradient resistance, acceleration resistance, and rolling resistance as opposed to the motion of vehicles [13]. The aforementioned factors significantly intensify the fuel consumption of automobiles and thereby the emission of GHGs [14]. Among these factors, rolling resistance is a crucial factor because it is governed by the texture and structural characteristics of pavements, the performance and structural properties of vehicle's tires [15–19]. Several studies have shown that rolling resistance is responsible for about 10 % – 30 % of a vehicle's fuel usage and carbon release [4,20,21]. Furthermore, the reduction of rolling resistance by using low-rolling resistance pavements and low-rolling resistance tires can diminish fuel usage by up to 20 % [22]. In addition, various investigations presented that lowering 10 % – 30 % of rolling resistance can provide fuel economy of 2 % – 6 %, depending on the driving conditions, pavement types, and tire types [23–27].

In order to gain a better understanding of rolling resistance, different studies have been performed to investigate rolling resistance from different perspectives [18,28,29]. For example, a lot of effort has been made to identify the correlation between rolling resistance and its influencing factors, such as construction factors of tires and surface texture of pavements [12,30,31]. In addition, numerous road authorities, tire manufacturers, and policymakers would be interested in understanding the influence of rolling resistance on fuel consumption. The latest data of research change in Google scholar trends and Scopus [32] indicates that the topic interest in rolling resistance and mitigation of carbon emissions has increased from the year 2016 to present, as shown in Fig. 1. However, to the best of the author's knowledge, publications containing a comprehensive explanation of rolling resistance and its impact on fuel consumption are still not available. To fill in this gap, this paper aims to conduct an extensive review on different aspects of rolling resistance and its influence on fuel consumption.

To make this paper easier to understand, different sections are arranged. The first section gives some background information about rolling resistance and its environmental impact. The second and third sections present the commonly used definitions of rolling resistance and texture characterisation approaches of pavement surface. The fourth section discusses the influence of different factors on rolling resistance. The fifth and sixth sections review the field measuring methods and modelling approaches of rolling resistance. The seventh section summarises the methods which can be used to predict fuel consumption and environmental impact. The eighth section shows the conclusions of this paper and recommendations for future work. However, the benefit-cost analysis and the life cycle cost analysis of rolling resistance are beyond the scope of this paper. The work presented in this paper will help road authorities, tire manufacturers, and policymakers to gain more insight into rolling resistance and its environmental impact.

2. Definition of rolling resistance

To have a clear understanding of rolling resistance, definitions of rolling resistance from different perspectives are presented in this section.

2.1. Energy-based definition

Previously, rolling resistance has been defined as a force that resists the travelling of a tire in a particular direction [34]. However, this concept is valid only when a tire freely rolls on a flat surface and not that appropriate when a tire rolls on an uneven surface. Hence, considering the concepts of adhesion and hysteresis, it is preferable to define the rolling resistance as the energy loss per distance travelled [17]. In the scientific community of tires, the rolling resistance is normally defined based on the energy loss in the rubber compound of a rolling tire [35–38]. However, when a tire rolls on the surface of an asphalt pavement, the energy loss in the whole system can be divided into three main categories: (1) energy loss in the rubber compound of the tire, (2) energy loss in the asphalt pavement, and (3) energy loss in the suspension system of the tire [39–41].

When a tire rolls on a pavement surface, it can have different types of deformations, as shown in Fig. 2. These deformations have some unrecoverable components because of the inelastic rubber compounds in the tire [30,42]. The unrecoverable deformations are caused by the conversion of the stored energy in the tire to heat, which finally contributes to the total energy loss in defining rolling resistance [42,43]. According to the explanations of Li & West [38], a high amount of energy loss can be expected in the crown area of the tire, where a significant amount of tread compound is present. Furthermore, they emphasised that friction between polymer chains and the existence of reinforcing fillers of tread compound are the main causes to amplify the energy dissipation due to the deformation of tires. Therefore, according to the aforementioned authors, the material compounds used in crown area are more prone to energy loss and thereby trigger the rolling resistance.

Moreover, when a tire rolls on the surface of an asphalt pavement, the deformation of the pavement also contains unrecoverable components because the asphalt layer has viscous damping and other layers have hysteretic damping [42,44]. The unrecoverable deformation of the asphalt pavement also corresponds to energy dissipation, which contributes to the total energy loss. This part of rolling resistance caused by the structural deformation of pavements is usually termed as structural rolling resistance (SRR) [43]. In addition, when a tire rolls on an uneven pavement surface, the tire and wheel will vibrate up and down. In this process, the shock absorber in the suspension system also dissipates some energy, which contributes to the total energy loss in defining

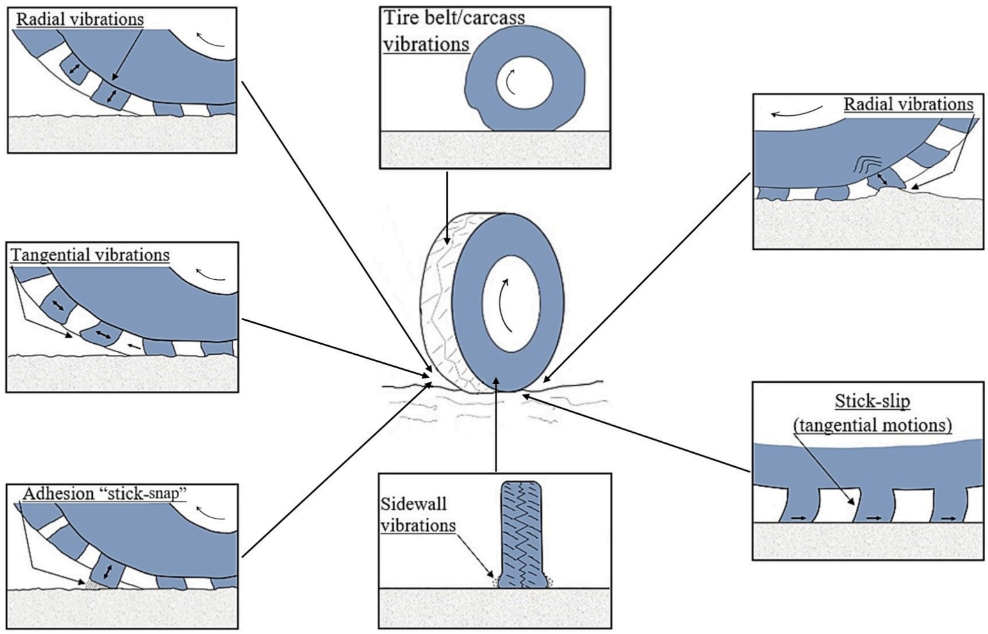

Fig. 2. Different types of deformation in the rolling process of a tire [42].

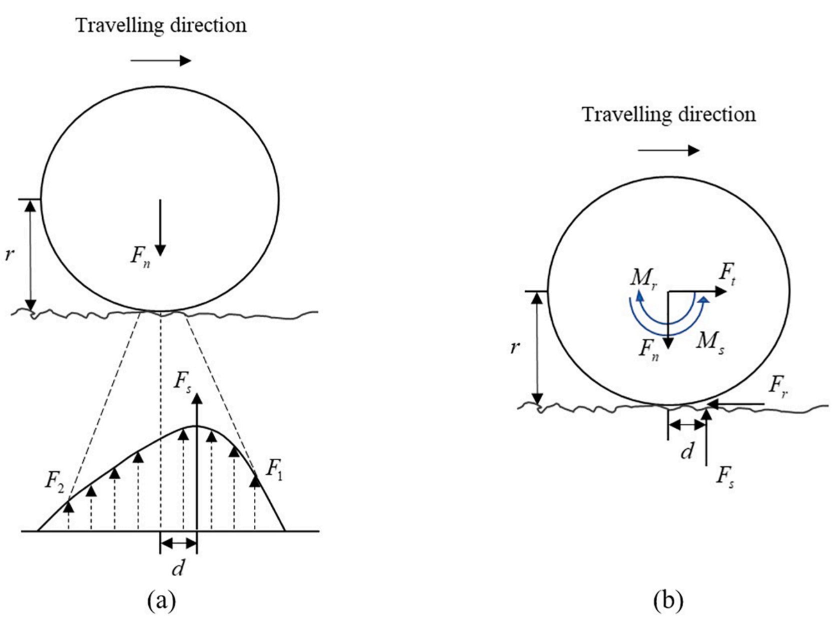

Fig. 3. Forces and moments acting on a rolling tire [48].

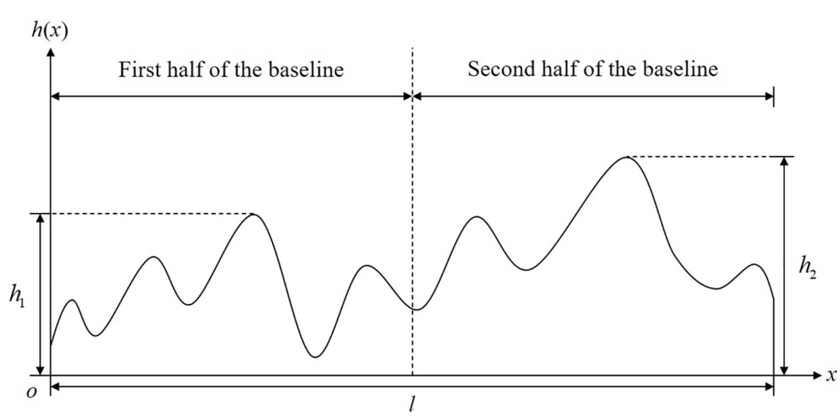

Fig. 4. Schematic representation of the texture profile of pavement surface.

rolling resistance [42].

2.2. Force-based definition

The aforementioned description gives a definition of rolling resistance from the perspective of energy dissipation. However, measuring force is more convenient than measuring energy in practice. Hence, the force-based definition of rolling resistance was also proposed in literature [35,41,45].

Assume that a tire subjected to a normal force F_n is rolling on a pavement, the forces and moments acting on the tire are shown in Fig. 3. Because of the inelasticity of the tire tread and the asphalt layer, the contact force between the rolling tire and the pavement surface are eccentrically distributed, as shown in Fig. 3(a). Due to this asymmetric force distribution, the resultant supporting force F_s acts on a point which has a distance d away from the symmetric line of the tire. Consequently, as shown in Fig. 3(b), the supporting force generates a moment M_s in the counterclockwise direction with the following magnitude:

$$M_s = F_s \cdot d \tag{2.1}$$

In order to balance this moment of eccentricity, it is necessary to apply a traction force F_t and a rolling resistance F_r, as shown in Fig. 3(b). The rolling resistance generates a moment M_r in the clockwise direction with the following magnitude:

$$M_r = F_r \cdot r \tag{2.2}$$

where r is the radius of the tire. To ensure that the tire rolls with a constant speed, the forces and moments should be balanced, i.e. $F_n = F_s$, $F_t = F_r$, and $M_s = M_r$. On the basis of these equalities, a dimensionless quantity called rolling resistance coefficient (RRC) is defined to characterise the rolling resistance in practice [35,41,46,47]:

$$\mathrm{RRC} = \frac{F_t}{F_n} \tag{2.3}$$

3. Texture characterisation of pavement surface

There are different parameters and approaches that can be used to characterise the texture properties of pavement surface. In this section, some classical parameters and wavelength-oriented parameters for texture characterisation were introduced. In addition, details of some enveloping algorithms for texture characterisation were also presented.

3.1. Classical parameters

In general, parameters that are frequently used to assess the texture characteristics of a pavement surface are Mean Profile Depth (MPD), Root Mean Square (RMS), Skewness, International Roughness Index (IRI), and so on [49,50]. The details of these parameters will be presented in this part.

(1) Mean Profile Depth

The schematic representation of the texture profile of pavement surface is shown in Fig. 4, in which $h(x)$ is the height of the texture with respect to a baseline along the x-axis. On a baseline with length l (which is normally 100 mm), the Mean Profile Depth (MPD) is defined as follows:

$$\mathrm{MPD} = \frac{h_1 + h_2}{2} - \bar{h} \tag{3.1}$$

where h_1 is the peak texture hight in the first half of the baseline, h_2 is the peak texture hight in the second half of the baseline, and $\bar{h}$ is the average texture hight [51,52].

(2) Root Mean Square

Within an evaluation length l, the Root Mean Square (RMS) value of the texture profile is defined as follows [53]:

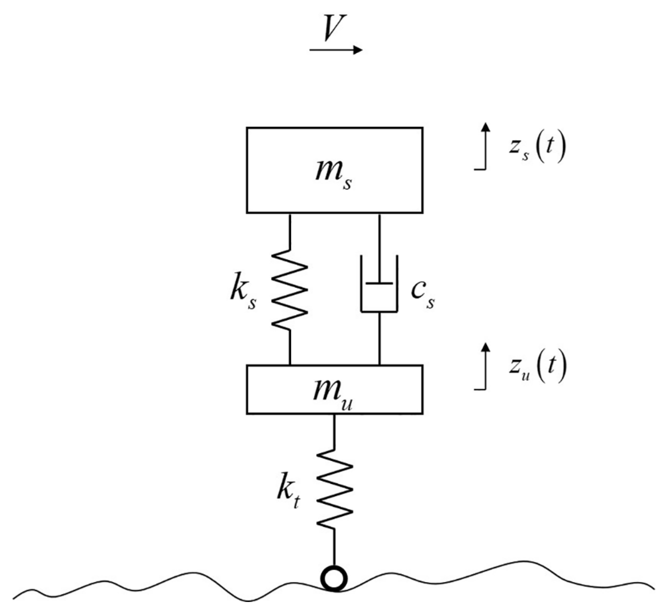

Fig. 5. Schematic representation of the quarter-car model [55,56].

$$\mathrm{RMS} = \sqrt{\frac{1}{l}\int_0^l h^2(x)dx} \tag{3.2}$$

(3) Skewness

Within an evaluation length l, the Skewness (RSK) of the texture profile is defined as follows [53]:

$$\mathrm{RSK} = \frac{1}{\mathrm{RMS}^3}\left[\frac{1}{l}\int_0^l h^3(x)dx\right] \tag{3.3}$$

(4) International Roughness Index

The definition of the International Roughness Index (IRI) is based on the response of a quarter-car model. The schematic representation of the quarter-car model is shown in Fig. 5, in which V is the forward speed which is often assumed as 80 km/h in the calculation of IRI, m_s is the sprung mass corresponding to the portion of vehicle body mass supported by one wheel, m_u is the unsprung mass corresponding to the mass of wheel, tire, and half of axle, c_s is the suspension damping rate, k_s is the suspension spring rate, k_t is the tire spring rate, $z_s(t)$ is the vertical displacement of the sprung mass, and $z_u(t)$ is the vertical displacement of the unsprung mass. Subsequently, the accumulated relative displacement between the sprung and unsprung masses in the quarter-car model normalised by the length l of the profile is defined as IRI [54]:

$$\mathrm{IRI} = \frac{1}{l}\int_0^{l/V} |\dot{z}_s(t) - \dot{z}_u(t)|dt \tag{3.4}$$

3.2. Wavelength-oriented parameters

The texture of pavement surface can be characterised by wavelength [57–62]. The texture with wavelength less than 0.5 mm is termed as micro-texture, the texture with wavelength between 0.5 mm and 50 mm is termed as macro-texture, the texture with wavelength between 50 mm and 0.5 m is termed as mega-texture, and the texture with wavelength between 0.5 m and 50 m is termed as unevenness. Basically, the micro-texture is related to mineralogy and petrology of aggregates, the macro-texture is related to the geometry and positioning of aggregates, and the unevenness is related to the longitudinal profile of pavement surfaces. Textures with different wavelengths have different effect on the vehicle-tire-pavement system, as shown in Fig. 6. In particular, textures which have influence on rolling resistance are unevenness, mega-texture, and

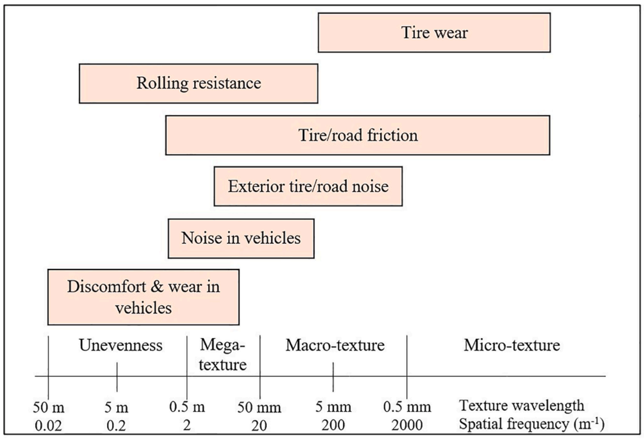

Note: The right sides of Tire/road friction and Exterior tire/road noise show a favorable effect of texture over this range, while Tire wear, Rolling resistance, Noise in vehicles, Discomfort & wear in vehicles, and the left sides of Tire/road friction and Exterior tire/road noise show an unfavorable effect.

Fig. 6. Effect of textures with different wavelengths [42].

macro-texture. The unevenness can be characterised by the parameter IRI and the macro-texture can be characterised by the parameter MPD, while the mega-texture is not well characterised by a certain parameter. Hence, an approach will be ideal if it can make use of the entire spectrum of the longitudinal road profile [63].

Furthermore, Goubert et al. [64] calculated the RMS value of the profile curve filtered by different bandpass filters to quantify texture of a pavement surface, these filters have passbands corresponding to different wavelengths. The measures of textures with different wavelengths can be represented by the following symbols: a_{Mi} for micro-texture, a_{Ma} for macro-texture, and a_{Me} for mega-texture. However, especially in noise-related studies, it is preferred to use the logarithms of these linear measures. These logarithm measures are expressed in dB relative to 1 μm RMS and represented by the following symbols: L_{Mi} for micro-texture, L_{Ma} for macro-texture, and L_{Me} for mega-texture. After filtering the profile curve by using filters with different passbands, the "spectral level" of each passband can be calculated. The most commonly used bandpass filters are one-third-octave bands [65]. As an example, a texture spectrum obtained by one-third-octave bands is shown in Fig. 7.

In addition, physical characteristics of pavement surface can also be used to characterise the texture of pavement surface, such as the geometric descriptors (e.g. peaks, valleys, and angles) extracted from pavement profiles [66] and the fractal dimension of pavement profiles [67–69]. The parameters mentioned above can be more meaningful if the pavement texture profile is pre-processed by using some enveloping algorithms, which will be introduced in the next part.

3.3. Enveloping algorithms

When a tire rolls on a pavement surface, it only envelops a part of the texture of pavement surface (especially for porous asphalt pavements). This implies that it is more reasonable to work on an enveloped texture profile obtained by using an enveloping algorithm [70]. The ideal enveloped texture profile should follow the deflection of the tire tread, and the enveloping algorithm can be an empirical algorithm or a physical model-based algorithm [71]. In what follows, three different enveloping algorithms are introduced.

(1) Algorithm of von Meier et al.

The algorithm proposed by von Meier et al. [72] is an empirical algorithm based on the mathematical limit of the second-order derivative of the discretised texture sample, which can be expressed as:

$$\frac{y_m - (y_{m-1} + y_{m+1})/2}{\Delta x^2} \leqslant d^* \tag{3.5}$$

where y_m is the magnitude of the m-th point of the profile, Δx is the sampling step, and d^* is the parameter which limits the second-order derivative of the enveloped profile. Physically, the parameter d^* characterises the tire stiffness and a value of 0.054 m^{-1} represents the average stiffness of car tires. By using this algorithm, a parabola shape penetration of the rubber into the texture cavities will be obtained.

(2) Algorithm of Clapp

The algorithm developed by Clapp [73] is based on a physical model, which focuses on evaluating the contact between a rigid body (indenter) and a semi-infinite elastic body. The rigid body represents the texture of pavement surface and the semi-infinite elastic body represents the rubber of tires. The semi-infinite elastic body is characterised by the Young's modulus E and the Poisson's ratio ν. For the characterisation of rubber materials, the Poisson's ratio ν can be set as 0.5. In the algorithm of Clapp, the considered problem is to find the displacement of the frontier of the elastic body caused by the indenter when a normal load is applied, as shown in Fig. 8.

For the semi-infinite elastic body, the vertical displacement $u(x)$ of the frontier caused by a pressure distribution $p(x)$ can be calculated by using the following equation:

$$\frac{\pi E u(x)}{2(1-\nu^2)} + c_0 = -\int_a^b p(\xi)\ln|\xi - x| d\xi \tag{3.6}$$

in which a and b are the limits of the contact zone, and c_0 is a constant to be determined. In addition, the global equilibrium of the system can be written as:

$$\frac{1}{b-a}\int_a^b p(x)dx = P \tag{3.7}$$

where P is the mean pressure applied on the semi-infinite elastic body.

There are two procedures in the algorithm of Clapp:

- The first procedure approximately calculates the texture-induced pressure distribution by using Equation (3.6) and assuming the rubber displacement $u(x)$ is known. In this procedure, the interface is discretised by using cubic splines and the pressure distribution is inversely determined from rubber displacement.
- The second procedure calculates the mean penetration depth of the rubber into texture asperities by using Equation (3.7) to obtain an approximated rubber displacement to be used in this approximation method.

(3) Algorithm of INRETS

The algorithm of INRETS [71] also considers the indentation problem shown in Fig. 8. For a semi-infinite elastic body subjected to a normal force δF at point $x = 0$, the vertical displacement $\delta u(x)$ of the frontier can be calculated by the following equation:

$$\delta u(x) = -\frac{2(1-\nu^2)}{\pi E}\ln|x|\delta F + \alpha \tag{3.8}$$

where α is a constant to be determined. According to the Green's formalism, the displacement at a point x with respect to the displacement at a reference point x_0 can be calculated as:

$$u(x) - u(x_0) = \int_C [g(x,\xi) - g(x_0,\xi)]p(\xi)d\xi \tag{3.9}$$

where $u(x)$ is the displacement at point x, C is the contact zone, $p(\xi)$ is the pressure distribution on C, and $g(x,\xi)$ is the Green's function of the problem which has the following expression:

$$g(x,\xi) = -\frac{2(1-\nu^2)}{\pi E}\ln|x-\xi| \tag{3.10}$$

In addition, the global equilibrium of the system can be expressed as:

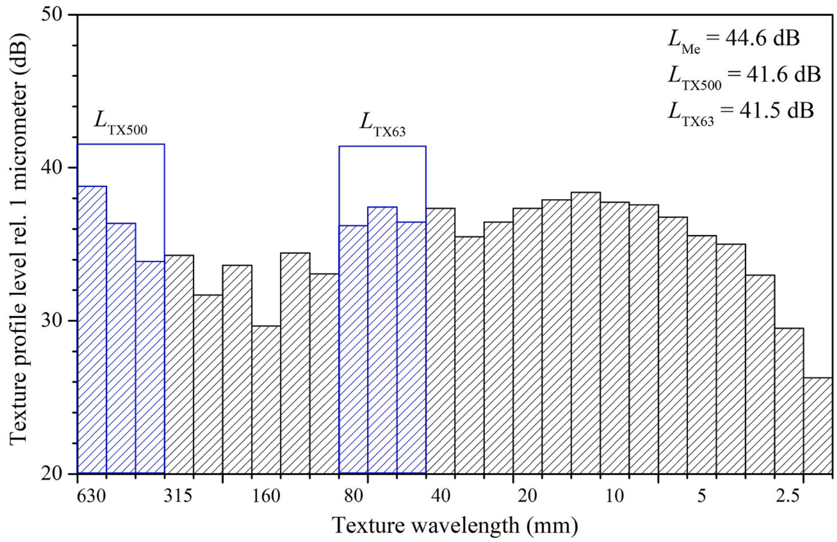

Fig. 7. A texture spectrum obtained by one-third-octave bands [64].

$$\frac{1}{L}\int_{C} p(x)dx = P \tag{3.11}$$

where L is the length of the sample and P is the mean pressure applied on the semi-infinite elastic body.

In this algorithm, the interface is first discretised into elements with equal length. Then, influence coefficients which give the displacement of each element when a unit force is applied on any element are calculated by Equation (3.9). At last, an iterative algorithm is used to determine the contact zone C, the pressure distribution $p(x)$, and the rubber displacement $u(x)$, which ensure that pressure is positive when contact occurs and the contact force balances the applied load. This algorithm can converge rapidly and guarantee a perfect fitting between the pressure distribution and the rubber displacement via Equation (3.9). As an example, the enveloped profiles for different types of pavement surface obtained by using the algorithm of INRETS are shown in Fig. 9, in which the parameter E is the Young's modulus of the tire rubber. It can be seen that the enveloped profile is closer to the original profile if the Young's modulus of the tire rubber is smaller.

4. Influence of different factors on rolling resistance

The factors which have influence on rolling resistance can be classified as tire-related factors and pavement-related factors. The tire-related factors include loads applied on the tire, materials of the tire, geometry configurations of the tire, and so on. The pavement-related factors include pavement surface texture, pavement stiffness, pavement temperature, and so on. In this section, the influence of different factors on rolling resistance is presented.

4.1. Influence of tire-related factors

When a tire rolls on a pavement surface, the energy loss in the tire contributes to the rolling resistance [74–76]. It was mentioned by El-Zomor [77] that the magnitude of the energy loss in tires is affected by tire construction, rubber properties, operating conditions, and so on.

4.1.1. Tire construction

Tire construction can affect rolling resistance substantially [41]. For instance, Schuring [78] reported that switching from a bias-ply tire to a radial-ply tire of the same radius and material reduces rolling resistance by approximately 20 % or more due to the change of stiffness of the tire. The radial-ply tire has higher tread rigidity against distortion and smaller contact area, which result in lower rolling resistance.

4.1.2. Rubber properties

It was indicated by Tabor [79] that the tread contains most of inelastic materials in a tire, and the tread alone can contribute more than 50 % of energy loss in a tire. Hence, changing the properties of rubbers in the tire tread could be an effective method to reduce rolling resistance.

4.1.3. Geometry configurations

Aldhufairi & Olatunbosun [80] reported that the geometric properties (e.g. aspect ratio) of tires also have influence on rolling resistance. It was indicated that rolling resistance can be reduced by shortening and stiffening the tire sidewall, or changing the rim size of wheels. However, it should be noted that changing the geometry of a tire will inevitably impact the material and design features, which also have influence on

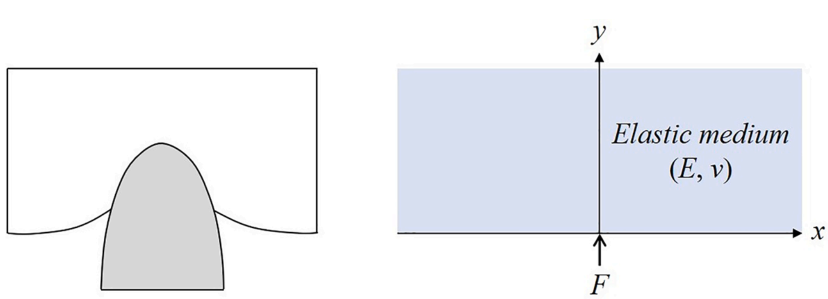

Fig. 8. The indentation problem considered in the algorithm of Clapp [73].

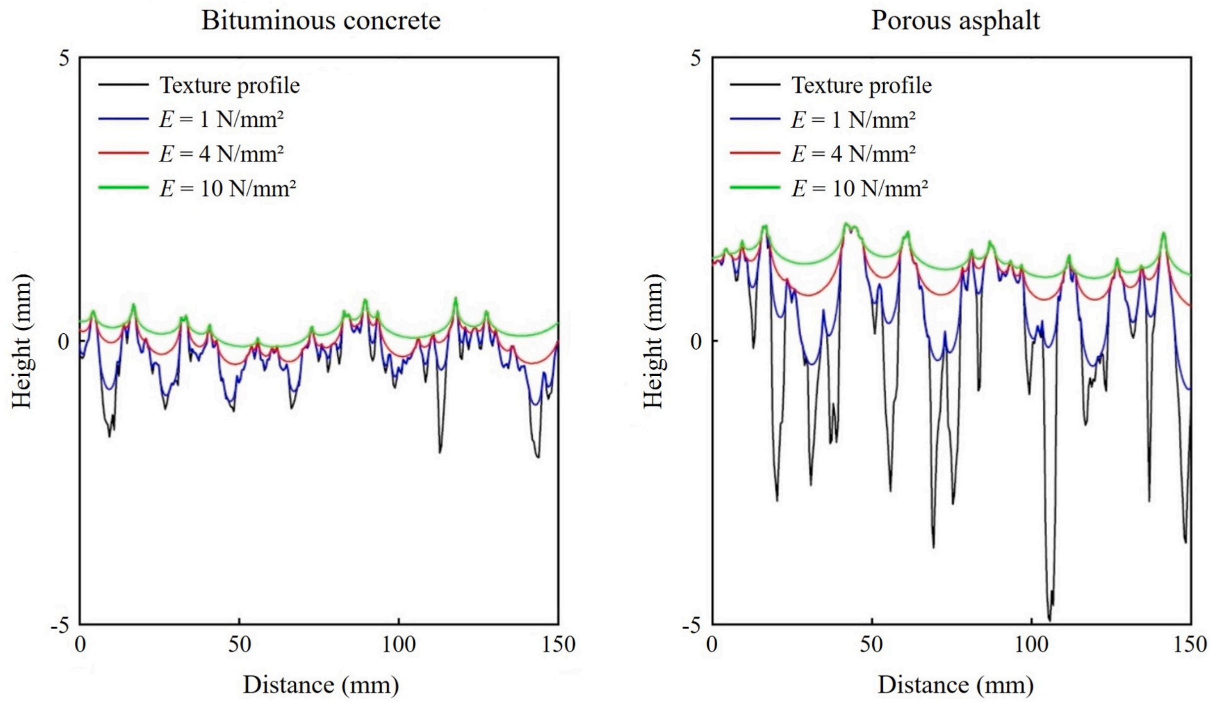

Fig. 9. Enveloped profiles obtained by using the algorithm of INRETS [71].

rolling resistance. Hence, it is difficult to know the specific magnitude of changes in rolling resistance caused by changes in tire dimensions.

4.1.4. Operating conditions

Rolling resistance can also be influenced by tire operating conditions, such as speed, axle load, and inflation pressure [38,81]. Li & West [38] and Nakajima [41] reported that increase in rolling resistance is observed when tires run at high speeds, which attributes to the high frequency of tire deformation. However, as speed increases, the temperature in the tire body also rises which will cancel out some of the increment in rolling resistance [22,28,81–83].

Furthermore, for a tire rolling with a certain speed, more applied axle loads will generate more deformations, which will result in more energy dissipation and higher rolling resistance. Studies of Gharibkhani et al. [84] and Transportation Research Board [85] found an approximately linear relationship between rolling resistance and sidewall deflection due to loads. Their findings showed that the increase in axle loads leads to a near-proportional increase in rolling resistance. Compared to passenger cars, the effect of axle loads on rolling resistance is more significant for trucks because of the relatively larger variation in axle loads of trucks.

In addition, inflation pressure also affects tire deformation and consequently affects rolling resistance [81,86]. Tires with lower inflation pressure exhibit more sidewall distortion, which eventually increases the rolling resistance. It is observed that for typical tires of passenger cars, an increase in inflation pressure from 165 kPa to 200 kPa will reduce rolling resistance by 10 %; and for a tire with inflation pressure between 165 kPa and 250 kPa, each drop of 7 kPa results in 1.4 % increase in rolling resistance [87]. Hence, maintaining optimal tire pressure is important in avoiding the increase of rolling resistance and reducing the unnecessary energy consumption of vehicles [88,89].

4.2. Influence of pavement-related factors

It was reported that rolling resistance is also significantly influenced by pavement-related factors, such as pavement surface texture, pavement stiffness, and pavement temperature [29,46,90].

4.2.1. Pavement surface texture

The surface texture of asphalt pavements has a significant influence on rolling resistance [91,92]. For example, Schmidt & Dyre [91] stated that 6 % – 30 % change in rolling resistance can be caused by the change of surface texture. It was indicated by Steyn & Ilse [21] that macro-texture has a significant effect on rolling resistance. Pavements with higher macro-texture lead to higher energy dissipation in the rubber material of tires and thereby higher rolling resistance [37,93,94]. The macro-textured surfaces have two different types, namely positively macro-textured surfaces and negatively macro-textured surfaces [95]. Positively macro-textured surfaces are produced by shaving and levelling the excessive height of aggregates. These surfaces have irregularities with apexes which can penetrate into the tread layer of tires. On the other hand, negatively macro-textured surfaces are produced by voids which are under the interface between tires and pavements. These surfaces have irregularities with cavities, but the tread layer of tires cannot penetrate into these cavities significantly and easily. Therefore, negatively macro-textured surfaces result in lower rolling resistance than positively macro-textured surfaces [96,97].

4.2.2. Pavement stiffness

It was reported by Mukherjee [90] that soft and rough surfaces result in higher rolling resistance than hard and smooth surfaces. For example, the study of van Haaster et al. [31] indicated that the double-layer porous asphalt concrete with aggregate size of 2/6 provides 8 % – 10 % lower rolling resistance than the single-layer porous asphalt concrete with aggregate size of 6/16. Researchers explained that pavements with high stiffness have smaller structural deflections than pavements with low stiffness, and thereby lower rolling resistance and less fuel consumption [29,98,99], especially under conditions of high temperature and heavy loading [100]. In addition, asphalt pavements which consist of small size aggregates have a low texture level, and thereby low rolling resistance when equipping enough tire-pavement contact [91,101].

4.2.3. Pavement temperature

Studies have shown that the ambient temperature and pavement temperature have a great effect on rolling resistance [46,102]. At high ambient temperature and pavement temperature, the overall temperature of tires will be increased and the modulus of the rubber material in tires will be decreased, which thereby reduces the energy dissipation in tires and lowers the rolling resistance [92].

4.2.4. Pavement wetness

It was found that pavement wetness has a significant influence on rolling resistance [103]. The rolling resistance of wet pavement surface is higher than that of dry pavement surface, and the increase of rolling resistance is influenced by the water film thickness. When the thickness of water film on pavement surface is less than 0.1 mm, the increase of rolling resistance is mainly caused by the decrease of tire temperature due to the cooling effect of water. When the thickness of water film on pavement surface is greater than 0.1 mm, the increase of rolling resistance is caused by both the cooling effect of water and the hydrodynamic phenomena that cause energy dissipation [104].

The reduction of rolling resistance is beneficial to improve fuel efficiency and relieve environmental impact of pavement-based conveyance. In order to reduce rolling resistance, the content presented above indicates that the following methods can be used in practice. From the perspective of tires, it is recommended to choose tires with low rolling resistance, remove unnecessary loads applied by vehicles, and maintain optimal tire pressure. From the perspective of pavements, it is recommended to use pavement surfaces with negative textures, use pavement structures with high stiffness, use pavement surfaces constructed with small size aggregates, and promptly repair damaged pavements. In addition, it should be noted that, when reducing rolling resistance, there should still be enough skid resistance to ensure vehicles can stop safely.

5. Field measurement of rolling resistance

In practice, rolling resistance can be measured by different methods, which can be categorised as the drum method, the trailer method, the coastdown method, the fuel consumption method, and so on [34,105].

5.1. The drum method

The drum method measures the rolling resistance in laboratory by using a rotational drum and a fixed tire. The drum generally has a steel surface, which can be equipped with replicas of real pavement surfaces. Drums with different diameters can be used to test the rolling resistance of either care tires or truck tires. In general, forces or angular decelerations are measured to calculate the rolling resistance [34].

5.2. The trailer method

The trailer method measures the rolling resistance by using a specially designed trailer towed by a vehicle. In general, forces or angles are recorded to calculate the rolling resistance coefficient. The trailer is equipped with the test tire, which can be a passenger car tire or a heavy truck tire; and the towing vehicle can be a passenger car or a truck. In addition, the trailer with the test tire can also be integrated into a truck to measure forces and moments of the tire under real operation conditions [34].

5.3. The coastdown method

The coastdown method measures the rolling resistance by using a vehicle. The rolling resistance is calculated based on the measured deceleration and other parameters of the vehicle when the vehicle freely rolls with the clutch being down and the gear being in the neutral position. In the application of this method, eliminating or compensating aerodynamic resistance and gravitational resistance is the main difficulty [106].

5.4. The fuel consumption method

The fuel consumption method calculates the rolling resistance by using a fuel consumption model or a rolling resistance model on the basis of the fuel consumption measured by specially instrumented vehicles. A variant of this method is the energy consumption method, in which an electric vehicle is used. However, the drawback of this method is that it is difficult to distinguish the contribution of rolling resistance from the contribution of other factors to the total fuel consumption or energy consumption [63].

According to these methods, different devices have been developed to measure the rolling resistance either directly or indirectly. Details of the commonly used measuring devices for rolling resistance (RR) are summarised in Table 1. For methods which conduct RR measurements in the laboratory (e.g. the drum method), the advantage is that the measuring conditions are controllable, while the disadvantage is that the measuring conditions can be unrepresentative which makes the obtained results far from the actual situation and unable to be used directly. For methods which conduct RR measurements in the field (e.g. the trailer method, the coastdown method, the fuel consumption method), the advantage is that the measuring conditions are realistic, while the disadvantage is that the measuring conditions are uncontrollable which introduces uncertainties in the measurements.

6. Modelling of rolling resistance

In literature, it was found that the rolling resistance can be investigated by either empirical modelling or computational modelling [108,113]. In empirical modelling approaches, the prediction of rolling resistance is usually performed based on experiments. In computational modelling approaches, the Finite Element Method (FEM)-based modelling of tire, pavement, and tire-pavement interaction are usually conducted with considering the concepts and laws of physics. The details about the empirical modelling and computational modelling of rolling resistance are presented in this section.

6.1. Empirical modelling

An effective way to study rolling resistance is to conduct experiments [114]. Many experimental studies have resulted in different empirical relationships between rolling resistance and texture parameters of pavement surface, which are reviewed in this part.

6.1.1. Relationships with RMS

In literature, experimental studies showed that RRC can be correlated with RMS (mm) in the following forms:

- Boere's experiment [115]:

$$RRC = 0.001 \cdot RMS + 0.0087 \tag{6.1}$$

- NCHRP project 1–45 [116]:

$$RRC = 0.0008 \cdot RMS + 0.0069 \tag{6.2}$$

- MIRIAM project [117]:

$$RRC = 0.003 \cdot RMS + 0.0108 \tag{6.3}$$

6.1.2. Relationships with MPD

Based on the field measurements conducted by the company M+P in 2013, Hooghwerff et al. [118] found the following relationship between RRC (kg/t) and MPD (mm):

$$RRC = 0.95 \cdot MPD + 7.92 \tag{6.4}$$

Table 1
Rolling resistance measuring devices.

Measuring devices	Measuring methods	Main parameters	Other parameters	References
Test drum equipped with replica of road surface at TUG	Method: The drum method; Type: Direct	Measure: RR coefficient	Tire type: Passenger car tires; Surface type: Epoxy resin- or polyurethane-based replica of road surface; Standard: ISO/TS 11819–3: 2017	[107]
External test drum for tires at TUG	Method: The drum method; Type: Direct	Measure: RR on tires	Tire type: Passenger car tires; Dimension of the drum: Diameter 1700 mm; Standard: ISO 28580	[92]
Internal test drum for tires at BASt	Method: The drum method; Type: Direct	Measure: RR on tires	Tire type: Passenger car tires and other tires; Standard: ISO 28580	[92]
Trailer R^2 Mk.2 built by TUG	Method: The trailer method; Type: Direct	Measure: RR coefficient	Tire type: Passenger car tires; Wheel load: 4150 N; Dimensions of the test wheel: Diameter 570–730 mm and width up to 245 mm; Tire pressure: 210 kPa; Standard: ISO/TS 11819–3: 2017	[22,108,109]
Trailer SRT-3	Method: The trailer method; Type: Indirect	Measuring speed: 60 km/h	Wheel load: 2943 N; Dimension of the test wheel: Diameter 645 mm; Standard: ISO 23671	[110]
Trailer FKA	Method: The trailer method; Type: Direct	Measure: RR coefficient; Measuring speed: 90 km/h	Tire type: Truck tires; Wheel load: 6000 N; Dimension of the test wheel: Diameter 560–1240 mm	[92]
Private car	Method: The coastdown method; Type: Indirect	Measures: Deceleration and other parameters of the vehicle	Tire type: Passenger car tires; Weight of the car: 1700 kg; Dimension of wheels: Diameter 762 mm; Standard: ISO 10521–1	[106]
Truck	Method: The fuel consumption method; Type: Indirect	Measure: Fuel consumption	Tire type: Truck tires; Weight of the truck: 13500 kg; Dimension of wheels: Diameter 1016 mm	[111]
Laser Crack Measurement System (LCMS)	Method: Others; Type: Indirect	Measure: Macro-texture; Measuring speed: 0–100 km/h; Sampling rate: 5600/28000 profiles/s; Measuring interval: 1–5 mm; Output profiles: 2D and 3D	Number of laser profilers: 2; Dimensions of laser profilers: 428 mm (h) × 265 mm (l) × 139 mm (w); Weight of laser profilers: 10 kg	[112]
Moving-rig machine	Method: Others; Type: Direct	Measure: RR coefficient	Tire type: Passenger car tires and other tires	[92]
Rolling-belt machine for tires at Calspan	Method: Others; Type: Direct	Measure: RR on tires	Tire type: Passenger car tires; Standard: ISO 28580	[92]
Moving ground machine for tires at VTI	Method: Others; Type: Direct	Measure: RR on tires	Tire type: Passenger car tires and other tires	[92]

Note: RR means rolling resistance and TUG means Gdańsk University of Technology.

6.1.3. *Relationships with MPD and RMS*

According to the field measurements conducted by the company M+P in 2013, Hooghwerff et al. [118] expressed RRC (kg/t) with texture parameters MPD (mm) and RMS (mm) in the following form:

$$\mathrm{RRC} = 0.99\cdot\mathrm{MPD} + 0.63\cdot\frac{\mathrm{MPD}}{\mathrm{RMS}} + 7.03 \tag{6.5}$$

6.1.4. *Relationships with MPD and IRI*

Past literature studies show that pavement parameters, such as MPD and IRI, have a significant influence on rolling resistance [119,120]. This effect has been considered in the development of different models, such as the Highway Development and Management Model-Version 4 (HDM-4) developed by the World Road Association (PIARC) and the model developed by the Swedish National Road and Transport Research Institute (VTI). The HDM-4 is a mechanistic-empirical model software tool which can be used for cost analysis of pavement maintenance and rehabilitation, and it contains a model for rolling resistance prediction based on MPD and IRI [121]. Furthermore, according to the model developed by VTI, the rolling resistance for a car can be calculated by an equation which was developed mainly based on the empirical data from the coastdown and the drum measurements in Sweden [117]:

$$\mathrm{RR} = mg\cdot(0.00172\cdot\mathrm{MPD} + 0.000021\cdot\mathrm{IRI}\cdot V + 0.00912) \tag{6.6}$$

where RR is the rolling resistance (N), m is the vehicle mass (kg), V is the vehicle speed (m/s), MPD is the Mean Profile Depth (mm), and IRI is the International Roughness Index (m/km).

In addition, Sandberg et al. [119] proposed the following model to describe the influence of pavement surface on rolling resistance:

$$\mathrm{RRC} = 0.002\cdot\mathrm{MPD} + a\cdot\mathrm{IRI} + b \tag{6.7}$$

where a and b are constants to be determined. The value of b is about 0.008 to 0.012 for light vehicles and about 0.004 to 0.0072 for heavy vehicles.

It can be seen from the text above that different studies use different models to describe the influence of pavement surface properties on rolling resistance. The possible reasons are: (a) the contribution of pavement surface to rolling resistance is relatively small; (b) isolating and quantifying the effect of pavement surface on rolling resistance are difficult; (c) the measurement of rolling resistance depends on testing methods and testing conditions [117].

6.2. *Computational modelling*

In addition to the empirical modelling, the rolling resistance can also be investigated by the computational modelling. A commonly used method for the computational modelling of rolling resistance is the

Finite Element Method (FEM). According to previous studies, the development of finite element models for evaluating rolling resistance mainly involves three aspects, i.e. the modelling of tire, the modelling of asphalt pavement, and the modelling of tire-pavement interaction [122,123]. In this part, the approaches that are generally used for the computational modelling of tire, asphalt pavement, and tire-pavement interaction are discussed.

6.2.1. Tire

The modelling of tires is an important while complex task. The complexity of tire models is getting high when tending to develop detailed tire models [124,125]. However, building up a detailed tire model is necessary to accurately predict the response of tires. From the perspective of pavement analysis, the choice of a detailed tire model or a simplified tire model is still a dilemma.

Recently, Tchuigwa et al. [125] presented the significance of each tire component for the realistic and advanced numerical modelling of tires under dynamic loads; the study was extended to consider the component of rubber compounds, textile cords, and steel cords, and the functions of each element were discussed from the mechanical point of view. Generally, the tread layer (complex pattern, simplified pattern, or without pattern), sidewall, reinforcements (carcass, bead wires, and belts), and rim were considered for the modelling of tires. Most of the studies used tire models with simplified tread pattern or without tread pattern for their analyses to avoid excessive computational time [126–128]. Furthermore, the reinforcements were modelled as quadrilateral membrane rebar elements embedded in the rubber compounds. In addition, the rim was created as a rigid section and tie constraints were used to make connection between rim and rim rubber compound with bead wires [122,126,127].

As mentioned before, the rubber compounds in tires have inelastic properties. However, these rubber compounds are generally modelled as incompressible and hyper-elastic materials [129]. According to past studies, different types of constitutive models can be used to describe the mechanical behaviour of rubber compounds, e.g. the Mooney-Rivlin model, the Yeoh model, the Ogden model, the Neo-Hookean model, and the Marlow model [130,131].

6.2.2. Asphalt pavement

The numerical simulation of asphalt pavements is time and resource intensive, especially when considering the surface texture and the whole pavement structure. The consideration of surface texture in the numerical simulation of pavements is important to predict behaviour related to tire-pavement interaction [123,132]. The texture of pavement surface can be reconstructed in the numerical simulation by using different methods, such as the laser scanning and the computed tomography (CT) scanning incorporating segmentation algorithms [123,133].

In addition, to obtain accurate response of pavements, the numerical simulation should consider all the pavement layers, such as the asphalt layer, the base layer, and the subgrade. The surface layer of asphalt pavements is composed of asphalt mixtures, which mainly contain aggregates, bitumen, and fillers. These components express different mechanical characteristics in asphalt mixtures, such as aggregates exhibit elasticity and bitumen exhibit viscoelasticity. To describe the mechanical characteristics of asphalt pavements, different constitutive models have been developed in previous studies [133–135]. In numerical simulations, the asphalt layer is generally considered to be purely elastic or viscoelastic, while the other layers are usually considered to be purely elastic [136–138]. Because of the viscoelasticity of asphalt layers, asphalt pavements are extremely responsive to loading frequencies and temperature levels [133]. By using proper constitutive models, the response of the whole pavement structure under different loading conditions can be investigated [113,139,140].

6.2.3. Tire-pavement interaction

In literature, many researchers used the FEM to investigate the rolling resistance caused by tire-pavement interaction. For example, Shida et al. [141] proposed a method to calculate the tire rolling resistance based on a static finite element model, this method needs short computational time and fulfils adequate accuracy. Luchini et al. [142] developed a quasi-static finite element model to predict tire rolling resistance, where a strain-based material model was used to describe the behaviour of rubber materials. Mars & Luchini [143] developed a model to predict the transient rolling resistance of tires, while the effect of tire inflation pressure and operating temperature was not considered.

Furthermore, Lu et al. [144] developed a finite element model to quantify the energy dissipation in a pavement under a rolling wheel, which concluded that both the stiffness of the pavement and the speed of the rolling wheel affect the total energy dissipation. Pouget et al. [145] used a finite element model along with a linearly viscoelastic material model to quantify the dissipated energy in typical French pavements and calculated the vehicle fuel consumption on the basis of energy dissipation; the influence of vehicle travelling speed, temperature, and base layer thickness on the energy dissipation was also evaluated. Bazi et al. [146] developed a finite element model to calculate the rolling resistance from the perspective of energy loss by using the difference of surface deflections in front of and behind the tire pressure, which is mainly caused by the viscoelasticity of the asphalt layer. However, the above studies did not consider the effect of texture characteristics of pavement surface; and the tire loading was ideally represented by a moving load patch with uniformly distributed normal pressure, which means the realistic contact stresses on the tire-pavement interface were neglected.

Moreover, Shakiba et al. [14] proposed a tire-pavement interaction finite element model to evaluate the rolling resistance and fuel consumption caused by pavement structural deflections; a moving non-uniformly distributed load was considered to represent the tire-pavement contact stresses and the effect of different parameters (e.g. vehicle speed, pavement material properties, and pavement temperature) on rolling resistance was investigated. However, this model did not consider the energy loss from tires and was not validated by field measurements. Hernandez et al. [30] developed a finite element model to investigate the rolling resistance between truck tires and pavements at different tire operating conditions and temperatures, as shown in Fig. 10(a). However, this model simply considered the pavement as a flat rigid surface, as a result of which the effect of the pavement surface texture and the pavement layer deformation on rolling resistance was neglected.

Srirangam et al. [46] developed a three-dimensional finite element model to study the rolling resistance between car tires and asphalt pavements at different operating conditions based on a thermo-mechanical contact algorithm, as shown in Fig. 10(b). In this study, the real texture information of different asphalt pavement surfaces was incorporated into the pavement finite element sub-model and the rolling resistance was calculated based on the hysteretic energy loss in the tire. However, this study considered the pavement surface to be non-deformable and did not include the layered structure of pavements, which means that the contribution of pavement deformation to rolling resistance was neglected. Furthermore, the developed model is also computationally tedious and significantly time-consuming.

In addition, Rajaei & Chatti [147] developed a 3D finite element tire model to evaluate the effect of pavement macro-texture on rolling resistance, in which the macro-texture of pavement surface was characterised by the parameter RMS. This study indicated that RRC and RMS (mm) have the following relationship:

$$\mathrm{RRC} = 0.0012 \cdot \mathrm{RMS} + 0.0088 \tag{6.8}$$

It can be found from the aforementioned studies that the FEM is a powerful approach for the computational modelling of rolling resis-

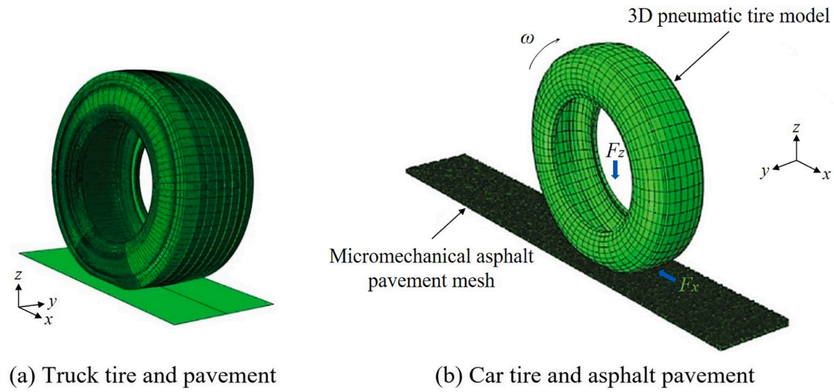

Fig. 10. Finite element modelling of tire-pavement interaction [30,46].

tance, but it still has some drawbacks. For instance, the FEM-based modelling generally cannot consider all the energy loss in the vehicle-tire-pavement system because of the difficulties in modelling and high computational costs, which affects the accuracy of the modelled results of rolling resistance.

7. Prediction of fuel consumption and environmental impact

As shown in Fig. 11, when a vehicle is moving on a pavement surface, it will experience different kinds of resistance [148]:

- Rolling resistance;
- Aerodynamic drag;
- Internal friction;
- Inertial force when there is acceleration;
- Gravitational force when driving in slopes.

The summation of these kinds of resistance is termed as driving resistance, which is related to the fuel consumption of vehicles. It should be highlighted that the rolling resistance only contributes to a part of the fuel consumption of vehicles.

By using a multi-parameter regression analysis, it is possible to separate and compare the contribution of different components to driving resistance. For example, Sandberg et al. [34] compared different components of driving resistance for a car and a heavy truck, the corresponding results are shown in Fig. 12, which indicates that:

- Only the air drag and the IRI-related component significantly depend on the driving speed;
- The air drag is very important for a car and less important for a heavy truck;
- The IRI-related component is significantly smaller than the MPD-related component for a car, while the IRI-related component is relatively important for a heavy truck.

In literature, different studies used different methods to predict the fuel consumption of vehicles. For example, the model developed by VTI contains a fuel consumption model that was formulated based on driving resistance. The fuel consumption model was calibrated by using values calculated from a theoretical model called VETO, which can calculate fuel consumption and exhaust emissions from traffic. According to the model developed by VTI, the fuel consumption of a car can be calculated by the following equation [117]:

$$\mathrm{FC} = 0.286\cdot\begin{pmatrix} 0.0394\cdot\mathrm{MPD} + 0.000481\cdot\mathrm{IRI}\cdot V \\ +0.0000807\cdot\mathrm{ADC}\cdot V^2 + 0.000667\cdot V^2 \\ +0.000297\cdot\mathrm{RG}^2 - 0.00611\cdot\mathrm{RG} + 1.209 \end{pmatrix}^{1.163}\cdot V^{0.056} \tag{7.1}$$

where FC is the fuel consumption (L/10 km), ADC is the average degree of curvature (rad/km), and RG is the road gradient (m/km). In addition, in order to quantify the effect of a certain change in rolling resistance on the change in fuel consumption, a parameter called return factor (RF) with the following definition can be used [78]:

$$\mathrm{RF} = \frac{\Delta \mathrm{FC}}{\Delta \mathrm{RR}} \tag{7.2}$$

where ΔFC means the change in fuel consumption and ΔRR means the change in rolling resistance.

Previous studies show that the environmental cost of pavements during the whole life cycle is significantly impacted by the pavement surface properties [149–151]. The reason is that pavement surface properties (e.g. MPD and IRI) can affect the fuel consumption of vehicles

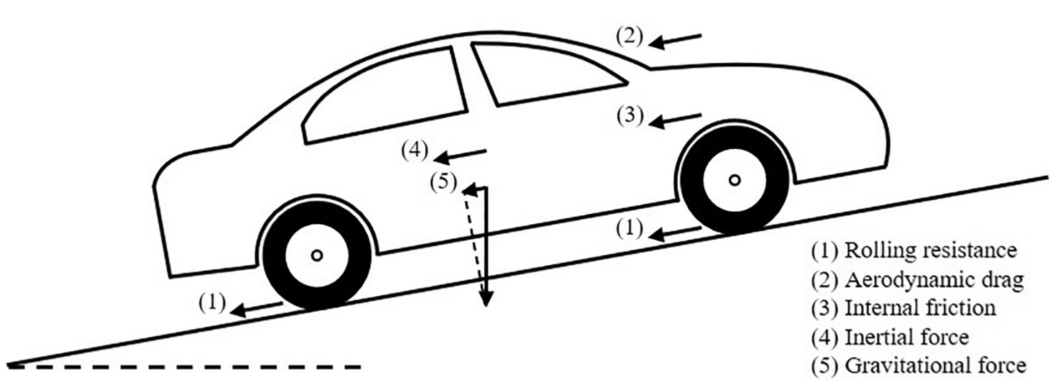

Fig. 11. Illustration of different components of driving resistance of vehicles.

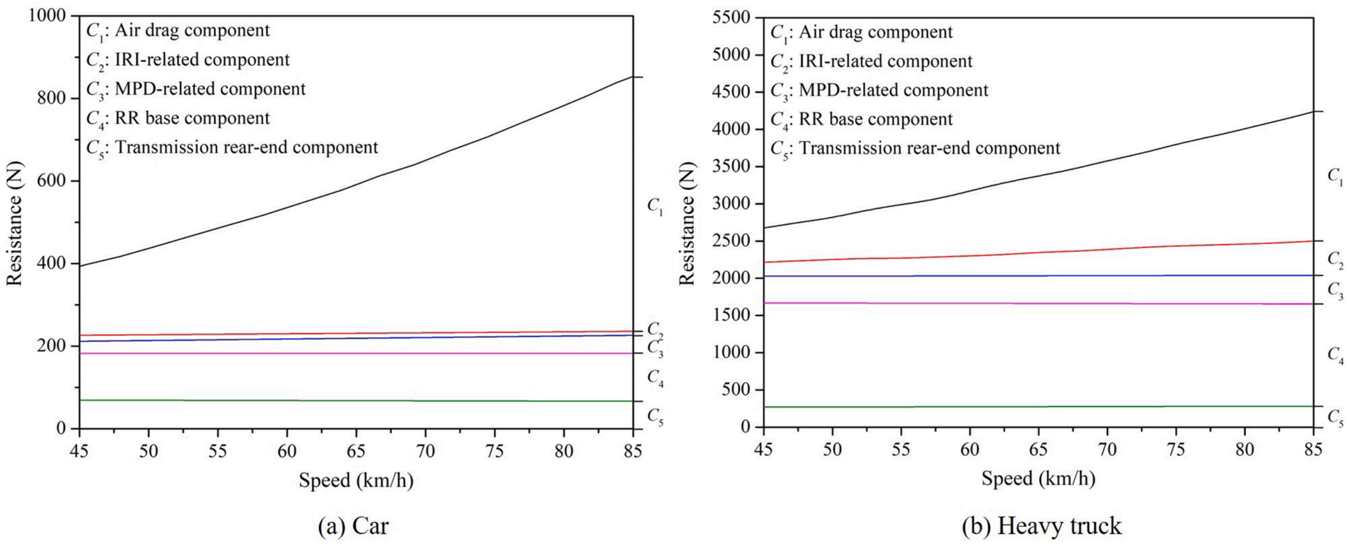

Fig. 12. Comparison of different components of driving resistance [34].

and further affect the exhaust emission of vehicles. In the approach developed by Wang et al. [151,152] at the University of California Pavement Research Centre (UCPRC, Davis), the HDM-4 was employed to estimate rolling resistance and the MOVES (Motor Vehicle Emission Simulator) [153] was employed to convert rolling resistance to vehicle emission. The HDM-4 was calibrated for U.S. conditions and the MOVES is the highway vehicle emission model developed by the U.S. Environmental Protection Agency (EPA) based on national data. By using this approach, the following model was developed to predict vehicle emission:

$$T_{CO_2} = a_1 \cdot \text{MPD} + a_2 \cdot \text{IRI} + a_3 \tag{7.3}$$

where T_{CO_2} is the tailpipe CO_2 emission factor; the terms a_1, a_2, and a_3 are the coefficients derived from the regression analysis, the values depend on the conditions of pavements and vehicles; MPD is the Mean Profile Depth (mm), and IRI is the International Roughness Index (m/km). In addition, the CO_2 emission of vehicles can also be calculated based on the fuel consumption by using the conversion process proposed by the International Carbon Bank & Exchange (ICBE) [154].

It should be highlighted that different methods can give totally different CO_2 emission related to pavement surface properties [150]. This is caused by the fact that the development of models of rolling resistance and fuel consumption is highly dependent on the formulating methods and the testing conditions.

8. Conclusions and recommendations

With the rising concerns of climate change and global warming, researchers are focusing on mitigating the environmental impact of transportation industries. One significant area of ongoing research is the reduction of rolling resistance, which presents a challenging task primarily due to the complex interaction processes between tires and pavements. In the perspective of authors, there is a need for a research paper that comprehensively summarises the advancements and challenges in this topic, which appears to be scarce according to popular scholarly search engines. To fill in this gap, this paper conducted a comprehensive review on the rolling resistance of asphalt pavements and its environmental impact. Based on this review, the following conclusions can be drawn:

- It is more reasonable to define rolling resistance from the perspective of energy, while the definition from the perspective of force is more suitable for practical applications;
- An ideal approach for texture characterisation of pavement surfaces is to make use of the entire wavelength spectrum of road profiles and consider the enveloping curve of tire treads;
- The rolling resistance can be influenced by different factors, which introduces difficulties in accurate measurement and modelling of rolling resistance;
- There are different devices to measure rolling resistance in practice, but the empirical relationships obtained from field measurements significantly depend on testing methods and conditions;
- In the computational modelling of rolling resistance, considering all the energy loss in the vehicle-tire-pavement system is difficult and time-consuming;
- The formulating methods and measuring conditions have significant effect on the prediction of energy consumption and environmental impact caused by rolling resistance.

In order to develop models which can accurately predict rolling resistance of asphalt pavements and its environmental impact, it is recommended to conduct the following work in the future:

- Find texture parameters which are more promising to be correlated with rolling resistance;
- Reduce the error and uncertainty in the measurements of rolling resistance;
- Use emerging techniques to accurately predict rolling resistance.

Funding

This work is financially supported by Rijkswaterstaat, Ministry of Infrastructure and Water Management, The Netherlands.

CRediT authorship contribution statement

Zhaojie Sun: Methodology, Investigation, Writing – original draft, Writing – review & editing. **W.A.A.S. Premarathna:** Writing – review & editing, Investigation. **Kumar Anupam:** Writing – review & editing, Supervision, Project administration, Conceptualization, Funding acquisition. **Cor Kasbergen:** Writing – review & editing, Supervision, Project administration, Funding acquisition. **Sandra M.J.G. Erkens:** Supervision, Project administration, Funding acquisition.

Declaration of Competing Interest

The authors declare that they have no known competing financial interests or personal relationships that could have appeared to influence the work reported in this paper.

Data availability

Data will be made available on request.

Acknowledgements

This paper is created under the research program Knowledge-based Pavement Engineering (KPE). KPE is a cooperation between Rijkswaterstaat, TNO, and TU Delft in which scientific and applied knowledge is gained about asphalt pavements and which contributes to the aim of Rijkswaterstaat to be completely climate neutral and to work according to the circular principle by 2030. The opinions expressed in this paper are solely from the authors.

References

[1] S. Alataş, Do environmental technologies help to reduce transport sector CO_2 emissions? Evidence from the EU15 countries, Res. Transp. Econ. 91 (2022) 101047, https://doi.org/10.1016/j.retrec.2021.101047.
[2] D.E. Shropshire, Life-cycle assessment of greenhouse gas emissions, Technology 8 (4–6) (2002) 167–180, https://doi.org/10.1007/978-3-030-72579-2_2.
[3] X. Yang, L. Liu, Analysis of the influence of passenger load on bus energy consumption a vehicle-engine combined model-based simulation framework, Sci. Rep. 12 (1) (2022) 14535, https://doi.org/10.1038/s41598-022-18866-6.
[4] C. Constantin, M. Băţăus, C. Renţea, G. Frăţilă, Effectiveness of the measures for CO_2 emission reduction in real world, IOP Conf. Ser.: Mater. Sci. Eng. 1220 (1) (2022) 12015, https://doi.org/10.1088/1757-899X/1220/1/012015.
[5] R. He, L. Luo, A. Shamsuddin, Q. Tang, Corporate carbon accounting: A literature review of carbon accounting research from the Kyoto Protocol to the Paris Agreement, Account. Finance 62 (1) (2022) 261–298, https://doi.org/10.1111/acfi.12789.
[6] UNFCCC. Adoption of the Paris agreement (2015).
[7] S. Solaymani, CO_2 emissions patterns in 7 top carbon emitter economies: The case of transport sector, Energy 168 (2019) 989–1001.
[8] IEA. World energy outlook 2022, IEA, Paris, France, 2022.
[9] O. Edenhofer, Climate change 2014: Mitigation of climate change (Vol. 3), Cambridge University Press (2015).
[10] H. Ritchie, P. Rosado, M. Roser, Emissions by sector. Our World in Data (2020). [Online]. Available: https://ourworldindata.org/emissions-by-sector.
[11] European Union, EU transport in figures - Statistical pocketbook 2022, 2022.
[12] S. Pálinkás, Á. Tóth, Development of a measurement method to determine rolling resistance, IOP Conf. Ser.: Mater. Sci. Eng. 1237 (1) (2022) 012013, https://doi.org/10.1088/1757-899x/1237/1/012013.
[13] A. Kawakami, T. Ishigaki, Y. Shirai, M. Terada, K. Kubo, Evaluation method of pavement surface characteristics for rolling resistance, Road Mater. Pavement Des. 18 (sup2) (2017) 2–11, https://doi.org/10.1080/14680629.2017.1304264.
[14] M. Shakiba, H. Ozer, M. Ziyadi, I.L. Al-Qadi, Mechanics based model for predicting structure-induced rolling resistance (SRR) of the tire-pavement system, Mech. Time-Depend. Mater. 20 (4) (2016) 579–600, https://doi.org/10.1007/s11043-016-9313-0.
[15] K. Chow, Improving vehicle rolling resistance and aerodynamics, in: R. Folkson, S. Sapsford (Eds.), Alternative Fuels and Advanced Vehicle Technologies for Improved Environmental Performance, Second Edition, Woodhead Publishing, 2022, pp. 459–481, https://doi.org/10.1016/B978-0-323-90979-2.00009-3.
[16] J. Ejsmont, S. Sommer, Selected aspects of pavement texture influence on tire rolling resistance, Coatings 11 (7) (2021), https://doi.org/10.3390/coatings11070776.
[17] A.N. Gent, J.D. Walter, The pneumatic tire. National Highway Traffic Safety Administration (2006).
[18] Y. Shirai, A. Kawakami, M. Terada, K. Himeno, Evaluation of the CO_2 reduction effect of low rolling resistance asphalt pavement using the fuel consumption simulation method, in: International Road Federation World Meeting & Exhibition, Springer, Cham, 2022, pp. 589–601.
[19] X. Zhai, Y. Chen, D. Han, J. Zheng, X. Wu, Z. Wang, X. Li, X. Ye, L. Zhang, New designed coupling agents for silica used in green tires with low VOCs and low rolling resistance, Appl. Surf. Sci. 558 (2021) 149819, https://doi.org/10.1016/j.apsusc.2021.149819.
[20] J. Barrand, J. Bokar, Reducing tire rolling resistance to save fuel and lower emissions 2008-01-0154, SAE Int. J. Passeng. Cars - Mech. Syst. 1 (1) (2009) 9–17.
[21] W.J.vdM. Steyn, M. Ilse, Evaluation of tire/surfacing/base contact stresses and texture depth, Int. J. Transp. Sci. Technol. 4 (1) (2015) 107–118, https://doi.org/10.1260/2046-0430.4.1.107.
[22] B. Świeczko-Żurek, G. Ronowski, J. Ejsmont, Tyre rolling resistance and its influence on fuel consumption, Combustion Engines 168 (2017) 62–67, https://doi.org/10.19206/ce-2017-110.
[23] G. Davis, California state fuel-efficient tire report: Volume II, California Energy Commission (2003).
[24] L.R. Evans , NHTSA tire fuel efficiency consumer information program development: Phase 2 - Effects of tire rolling resistance levels on traction, treadwear, and vehicle fuel economy (2009).
[25] X. Na, D. Cebon, Quantifying fuel-saving benefit of low-rolling-resistance tyres from heavy goods vehicle in-service operations, Transp. Res. Part D: Transp. Environ. 113 (2022) 103501, https://doi.org/10.1016/j.trd.2022.103501.
[26] J.F. Rushing, J.D. Doyle, A. Harrison, Significance of non-load related distresses on airfield asphalt pavements: Review of 25 years of pavement management data. In Proc. 12th Int. Society of Asphalt Pavements (ISAP) Conf. on Asphalt Pavements (2014) 253–261, https://doi.org/10.1201/b17219-39.
[27] A. Soica, A. Budala, V. Monescu, S. Sommer, W. Owczarzak, Method of estimating the rolling resistance coefficient of vehicle tyre using the roller dynamometer, Proc. Inst. Mech. Eng., Part D: J. Automob. Eng. 234 (13) (2020) 3194–3204, https://doi.org/10.1177/0954407020919546.
[28] K. Anupam, S.K. Srirangam, A. Scarpas, C. Kasbergen, M. Kane, Study of cornering maneuvers of a pneumatic tire on asphalt pavement surfaces using the finite element method, Transp. Res. Rec. 2457 (1) (2014) 129–139, https://doi.org/10.3141/2457-14.
[29] O. Chupin, J.-M. Piau, A. Chabot, Evaluation of the structure-induced rolling resistance (SRR) for pavements including viscoelastic material layers, Mater. Struct. 46 (4) (2013) 683–696, https://doi.org/10.1617/s11527-012-9925-z.
[30] J.A. Hernandez, I.L. Al-Qadi, H. Ozer, Baseline rolling resistance for tires' on-road fuel efficiency using finite element modeling, Int. J. Pavement Eng. 18 (5) (2017) 424–432, https://doi.org/10.1080/10298436.2015.1095298.
[31] B. van Haaster, E. Worrell, J.P.F. Fortuin, W.-J. van Vliet, Potential energy savings by reducing rolling resistance of Dutch road pavements, J. Mater. Civ. Eng. 27 (1) (2015) 04014101, https://doi.org/10.1061/(ASCE)MT.1943-5533.0000999.
[32] S.-P. Jun, H.S. Yoo, S. Choi, Ten years of research change using Google Trends: From the perspective of big data utilizations and applications, Technol. Forecast. Soc. Chang. 130 (2018) 69–87, https://doi.org/10.1016/j.techfore.2017.11.009.
[33] Google Trends (n.d.). Retrieved 2022, from https://trends.google.com/trends/.
[34] U. Sandberg, U. Hammarström, M. Haider, M. Conter, L. Goubert, A. Bergiers, K.-P. Glaeser, G. Schwalbe, M. Zöller, O. Boujard, R. Karlsson, J.A. Ejsmont, T. Wang, J.T. Harvey. Rolling resistance - Basic information and state-of-the-art on measurement methods, 2011.
[35] X. Gao, Y. Zhuang, S. Liu, High-speed 3D digital image correlation for measuring tire rolling resistance coefficient, Measurement 171 (2021) 108830, https://doi.org/10.1016/j.measurement.2020.108830.
[36] H. Hota, V. Oleksiuk, A. Pascu, P. Dani, B. Gálfi, I.R. Száva, S. Vlase, J. (Ioan) Szava, G. Popa, Investigations on the rolling friction coefficient's evaluation of uncovered steel parts (2016), https://doi.org/10.26649/musci.2016.109.
[37] M. Kane, E. Riahi, M.-T. Do, Tire/road rolling resistance modeling: Discussing the surface macrotexture effect, Coatings 11 (5) (2021), https://doi.org/10.3390/coatings11050538.
[38] Y. Li, R. West, Rolling resistance revisited, Tire Sci. Technol. 47 (2019), https://doi.org/10.2346/tire.19.150089.
[39] D. Balzarini, K. Chatti, I. Zaabar, A.A. Butt, J.T. Harvey, Mechanistic-based parametric model for predicting rolling resistance of concrete pavements, Transp. Res. Rec. 2673 (7) (2019) 341–350, https://doi.org/10.1177/0361198119847611.
[40] R.E. Kim, S. Kang, B.F. Spencer, H. Ozer, I.L. Al-Qadi, Stochastic analysis of energy dissipation of a half-car model on nondeformable rough pavement, J. Transp. Eng., Part B: Pavements 143 (4) (2017) 04017016, https://doi.org/10.1061/JPEODX.0000014.
[41] Y. Nakajima, Rolling resistance of tires, in: Advanced Tire Mechanics, Springer, 2019, pp. 931–1017, https://doi.org/10.1007/978-981-13-5799-2_13.
[42] U. Sandberg, J.A. Ejsmont, Tyre/road noise reference book, INFORMEX HB, 2002.
[43] N.R. Nielsen, K. Chatti, C.P. Nielsen, I. Zaabar, P.G. Hjorth, T. Hecksher, Method for direct measurement of structural rolling resistance for heavy vehicles, Transp. Res. Rec. 2674 (5) (2020) 371–380, https://doi.org/10.1177/0361198120915699.
[44] J. Ling, F. Wei, H. Chen, H. Zhao, Y. Tian, B. Han, Accelerated pavement testing for rutting evaluation of hot-mix asphalt overlay under high tire pressure, J. Transp. Eng., Part B: Pavements 146 (2) (2020) 04020009, https://doi.org/10.1061/jpeodx.0000157.
[45] T.B. Rhyne, S.M. Cron, A study on minimum rolling resistance, Tire Sci. Technol. 40 (4) (2012) 220–233.
[46] S.K. Srirangam, K. Anupam, C. Kasbergen, A. Scarpas, V. Cerezo, Study of influence of operating parameters on braking friction and rolling resistance, Transp. Res. Rec. 2525 (1) (2015) 79–90, https://doi.org/10.3141/2525-09.
[47] C. Wei, O. Olatunbosun, M. Behroozi, Simulation of tyre rolling resistance generated on uneven road, Int. J. Veh. Des. 70 (2016) 113, https://doi.org/10.1504/IJVD.2016.074415.
[48] M. Helexa, J. Kováč, J. Krilek, J. Melicherčík, T. Kuvik, Comparison of achieved rolling resistance values of two selected tires on a solid surface, Appl. Sci. 12 (4) (2022) 2251.
[49] Q.J. Li, Y. Zhan, G. Yang, K.C. Wang, Pavement skid resistance as a function of pavement surface and aggregate texture properties, Int. J. Pavement Eng. 21 (10) (2020) 1159–1169.

[50] N. Zuniga-Garcia, J.A. Prozzi, High-definition field texture measurements for predicting pavement friction, Transp. Res. Rec. 2673 (1) (2019) 246–260.
[51] A. Aavik, T. Kaal, M. Jentson, Use of pavement surface texture characteristics measurement results in Estonia, in: The XXVIII International Baltic Road Conference, Vilnius, Lithuania, 2013.
[52] S. Torbruegge, B. Wies, Characterization of pavement texture by means of height difference correlation and relation to wet skid resistance, J. Traffic Transp. Eng. (English Edition) 2 (2) (2015) 59–67.
[53] S. Chen, X. Liu, H. Luo, J. Yu, F. Chen, Y. Zhang, T. Ma, X. Huang, A state-of-the-art review of asphalt pavement surface texture and its measurement techniques, J. Road Eng. 2 (2) (2022) 156–180.
[54] M.W. Sayers, On the calculation of international roughness index from longitudinal road profile, Transp. Res. Rec. 1501 (1995).
[55] K. Xue, T. Nagayama, B. Zhao, Road profile estimation and half-car model identification through the automated processing of smartphone data, Mech. Syst. Sig. Process. 142 (2020), 106722.
[56] B. Zhao, T. Nagayama, IRI estimation by the frequency domain analysis of vehicle dynamic responses, Procedia Eng. 188 (2017) 9–16.
[57] ASTM E867. Standard terminology relating to vehicle-pavement systems (2012).
[58] ISO 13473-2. Characterization of pavement texture by use of surface profiles - Part 2: Terminology and basic requirements related to pavement texture profile analysis (2002).
[59] B. Mataei, H. Zakeri, M. Zahedi, F.M. Nejad, Pavement friction and skid resistance measurement methods: A literature review, Open J. Civ. Eng. 6 (04) (2016) 537.
[60] Permanent International Association of Road Congresses (PIARC), Report of the committee on surface characteristics, Proceedings of the 18th World Road Congress, World Road Congress, Brussels, Belgium, 1987, 1–43.
[61] Permanent International Association of Road Congresses (PIARC), International PIARC experiment to compare and harmonize texture and skid resistance measurements, World Road Congress, Brussels, Belgium, 1995.
[62] B. Sengoz, A. Topal, S. Tanyel, Comparison of pavement surface texture determination by sand patch test and 3D laser scanning, Period. Polytech. Civ. Eng. 56 (1) (2012) 73–78.
[63] L.G. Andersen, J.K. Larsen, E.S. Fraser, B. Schmidt, J.C. Dyre, Rolling resistance measurement and model development, J. Transp. Eng. 141 (2) (2015) 04014075, https://doi.org/10.1061/(ASCE)TE.1943-5436.0000673.
[64] L. Goubert, M.-T. Do, A. Bergiers, R. Karlsson, U. Sandberg, J. Maeck, State-of-the-art concerning texture influence on skid resistance, noise emission and rolling resistance, in: FP7 Project ROSANNE Deliverable D, 2014.
[65] Z. Liao, Z. Gan, J. Hu, J. Zhao, B. Zhou, J. Zhang, Comparative study of two typical one-third octave algorithms in substation noise analysis, Energy Rep. 8 (2022) 319–326.
[66] F. Anfosso-Lédée, M.-T. Do, Geometric descriptors of road surface texture in relation to tire-road noise, Transp. Res. Rec. 1806 (1) (2002) 160–167, https://doi.org/10.3141/1806-18.
[67] A.G. Kokkalis, G.H. Tsohos, O.K. Panagouli, Consideration of fractals potential in pavement skid resistance evaluation, J. Transp. Eng. 128 (6) (2002) 591–595, https://doi.org/10.1061/(ASCE)0733-947X(2002)128:6(591).
[68] O.K. Panagouli, A.G. Kokkalis, Skid resistance and fractal structure of pavement surface, Chaos, Solitons Fractals 9 (3) (1998) 493–505, https://doi.org/10.1016/S0960-0779(97)00085-4.
[69] M. Yeggoni, J.W. Button, D.G. Zollinger, Fractals of aggregates correlated with creep in asphalt concrete, J. Transp. Eng. 122 (1) (1996) 22–28, https://doi.org/10.1061/(ASCE)0733-947X(1996)122:1(22).
[70] L.G. Del Pizzo, L. Teti, A. Moro, F. Bianco, L. Fredianelli, G. Licitra, Influence of texture on tyre road noise spectra in rubberized pavements, Appl. Acoust. 159 (2020), 107080.
[71] P. Klein, J.-F. Hamet, Road texture and rolling noise: An envelopment procedure for tire-road contact. https://hal.archives-ouvertes.fr/hal-00546120.
[72] A. von Meier, G.J. van Blokland, G. Descornet. The influence of texture and sound absorption on the noise of porous road surfaces. PIARC 2nd International Symposium on Road Surface Characteristics, 1992, pp. 7–19.
[73] T.G. Clapp, Spectral correlation of the surface profile in the development of a tire and pavement interaction force model, North Carolina State University, 1983.
[74] H. Heisler, Advanced vehicle technology, Elsevier, 2002.
[75] A.J. Martyr, M.A. Plint, Engine testing: The design, building, modification and use of powertrain test facilities, Elsevier, 2012.
[76] J.P. Pauwelussen, Essentials of vehicle dynamics, Elsevier, 2014.
[77] H.M. El-Zomor, Real-time estimation of pneumatic tyre hysteresis loss, Int. J. Heavy Veh. Syst. 26 (2) (2019) 175–187, https://doi.org/10.1504/IJHVS.2019.098275.
[78] D.J. Schuring, The rolling loss of pneumatic tires, Rubber Chem. Technol. 53 (3) (1980) 600–727, https://doi.org/10.5254/1.3535054.
[79] D. Tabor, Hysteresis losses in the friction of lubricated rubber, Rubber Chem. Technol. 33 (1) (1960) 142–150, https://doi.org/10.5254/1.3542120.
[80] H.S. Aldhufairi, O.A. Olatunbosun, Developments in tyre design for lower rolling resistance: A state of the art review, Proc. Inst. Mech. Eng., Part D: J. Automob. Eng. 232 (14) (2018) 1865–1882, https://doi.org/10.1177/0954407017727195.
[81] J. Ejsmont, G. Ronowski, W. Owczarzak, S. Sommer, Temperature influence on tire rolling resistance measurements quality, Int. J. Automot. Technol. 23 (1) (2022) 109–123, https://doi.org/10.1007/s12239-022-0009-y.
[82] D.A. Glemming, P.A. Bowers, Tire testing for rolling resistance and fuel economy, Tire Sci. Technol. 2 (4) (1974) 286–311, https://doi.org/10.2346/1.2167190.
[83] M. Juhala, Improving vehicle rolling resistance and aerodynamics, in: R. Folkson (Ed.), Alternative Fuels and Advanced Vehicle Technologies for Improved Environmental Performance, Woodhead Publishing, 2014, pp. 462–475, https://doi.org/10.1533/9780857097422.2.462.
[84] M. Gharibkhani, A. Mardani, F. Vesali, Determination of wheel-soil rolling resistance of agricultural tire, Aust. J. Agric. Eng. 3 (1) (2012) 6–11, https://doi.org/10.3316/informit.339221483960541.
[85] Transportation Research Board, Tires and passenger vehicle fuel economy: Informing consumers, improving performance (No. 286), National Research Council (2006), https://doi.org/10.17226/11620.
[86] V.T. Nguyen, V.D. Nguyen, M. Bouteldja, Estimation of rolling resistance, tire temperature and inflation pressure of heavy-duty vehicle, Int. J. Mech. Eng. Robot. Res. 11 (4) (2022) 255–261.
[87] K. Holmberg, P. Andersson, A. Erdemir, Global energy consumption due to friction in passenger cars, Tribol. Int. 47 (2012) 221–234, https://doi.org/10.1016/j.triboint.2011.11.022.
[88] S. d'Ambrosio, R. Vitolo, Potential impact of active tire pressure management on fuel consumption reduction in passenger vehicles, Proc. Inst. Mech. Eng., Part D: J. Automob. Eng. 233 (4) (2019) 961–975, https://doi.org/10.1177/0954407018756776.
[89] E. Pike, Opportunities to improve tire energy efficiency (2011).
[90] D. Mukherjee, Effect of pavement conditions on rolling resistance, Am. J. Eng. Res. 3 (7) (2014) 141–148.
[91] B. Schmidt, J.C. Dyre, CO_2 emission reduction by exploitation of rolling resistance modelling of pavements, Procedia. Soc. Behav. Sci. 48 (2012) 311–320, https://doi.org/10.1016/j.sbspro.2012.06.1011.
[92] L. Ydrefors, M. Hjort, S. Kharrazi, J. Jerrelind, A. Stensson Trigell, Rolling resistance and its relation to operating conditions: A literature review, Proc. Inst. Mech. Eng., Part D: J. Automob. Eng. 235 (12) (2021) 2931–2948, https://doi.org/10.1177/09544070211011089.
[93] K. Anupam, S.K. Srirangam, A. Scarpas, C. Kasbergen, Influence of temperature on tire-pavement friction: Analyses, Transp. Res. Rec. 2369 (1) (2013) 114–124, https://doi.org/10.3141/2369-13.
[94] Y. Ding, H. Wang, J. Qian, H. Zhou, Evaluation of tire rolling resistance from tire-deformable pavement interaction modeling, J. Transp. Eng., Part B: Pavements 147 (3) (2021) 04021041, https://doi.org/10.1061/JPEODX.0000295.
[95] T. Vieira, U. Sandberg, S. Erlingsson, Negative texture, positive for the environment: Effects of horizontal grinding of asphalt pavements, Road Mater. Pavement Des. 22 (1) (2021) 1–22.
[96] Finnish Transport Agency, The effect of road texture on road users and road maintenance, Road Department (2010).
[97] A. Woodside, D. Woodward, P. McErlean, Rolling resistance of surface materials affected by surface type, tyre load and inflation pressure, Maintenance and Rehabilitation of Pavements and Technological Control, Guimaraes, Portugal, 2003 https://trid.trb.org/view/684959.
[98] C.J. Bester, Effect of pavement type and condition on the fuel consumption of vehicles, Transp. Res. Rec. 1000 (1984) 28–32.
[99] G. Taylor, J. Patten, Effects of pavement structure on vehicle fuel consumption, Centre for Surface Transportation Technology (CSTT), 2006.
[100] A. Vashisth, R. Kumar, Review on effect of pavement characteristics on fuel consumption, Int. J. Eng. Adv. Technol. 7 (4) (2018) 129–138.
[101] S.W. Boere, G.J. van Blokland. Influence of road surface properties on rolling resistance of car tyres, M+P Consulting Engineers BV, 2008.
[102] J. Ejsmont, S. Taryma, G. Ronowski, B. Swieczko-Zurek, Influence of temperature on the tyre rolling resistance, Int. J. Automot. Technol. 19 (1) (2018) 45–54, https://doi.org/10.1007/s12239-018-0005-4.
[103] A. Carlson, T. Vieira, The effect of water and snow on the road surface on rolling resistance, Statens väg-och transportforskningsinstitut (2021).
[104] J. Ejsmont, L. Sjögren, B. Świeczko-Żurek, G. Ronowski, Influence of road wetness on tire-pavement rolling resistance, J. Civ. Eng. Archit. 9 (11) (2015) 1302–1310.
[105] Y. Huang, H. Chen, Review of rolling resistance influence on fuel consumption of trucks. In 13th ITS European Congress, Brainport, The Netherlands (2019).
[106] R. Karlsson, U. Hammarström, H. Sörensen, O. Eriksson, Road surface influence on rolling resistance: Coastdown measurements for a car and an HGV. Statens väg-och transportforskningsinstitut. http://urn.kb.se/resolve?urn=urn:nbn:se:vti:diva-554.
[107] G. Ronowski, Design and calibration of rolling resistance test trailer R^2Mk.2, IOP Conf. Ser.: Mater. Sci. Eng. 148 (1) (2016), 012026, https://doi.org/10.1088/1757-899X/148/1/012026.
[108] J.A. Ejsmont, G. Ronowski, B. Świeczko-Żurek, S. Sommer, Road texture influence on tyre rolling resistance, Road Mater. Pavement Des. 18 (1) (2017) 181–198, https://doi.org/10.1080/14680629.2016.1160835.
[109] J. Ejsmont, S. Taryma, G. Ronowski, B. Swieczko-Zurek, Influence of load and inflation pressure on the tyre rolling resistance, Int. J. Automot. Technol. 17 (2) (2016) 237–244, https://doi.org/10.1007/s12239-016-0023-z.
[110] J. Pytka, P. Budzyński, P. Tarkowski, M. Piaskowski, A portable wheel tester for tyre-road friction and rolling resistance determination, IOP Conf. Ser.: Mater. Sci. Eng. 148 (2016), 012025, https://doi.org/10.1088/1757-899X/148/1/012025.
[111] E. de Graaff, E. van Gils, Influence of road surface type on fuel consumption of trucks, M+P Consulting Engineers BV (2017).
[112] Pavemetrics | Laser Crack Measurement System (LCMS). (n.d.). Pavemetrics. Retrieved August 30, 2022, from https://www.pavemetrics.com/applications/road-inspection/lcms2-en/.
[113] Y. Kim, S. Lee, Experiments and numerical analysis of cold-recycled asphalt mixture modified with desulfurization gypsum additive, Constr. Build. Mater. 326 (2022), 126803, https://doi.org/10.1016/j.conbuildmat.2022.126803.
[114] B. Świeczko-Żurek, P. Jaskula, J.A. Ejsmont, A. Kędzierska, P. Czajkowski, Rolling resistance and tyre/road noise on rubberised asphalt pavement in Poland, Road

Mater. Pavement Des. 18 (1) (2017) 151–167, https://doi.org/10.1080/14680629.2016.1159245.
[115] S. Boere, Prediction of road texture influence on rolling resistance, Eindhoven University of Technology, 2009.
[116] K. Chatti, I. Zaabar, Estimating the effects of pavement condition on vehicle operating costs, Transportation Research Board, 2012.
[117] U. Hammarström, J. Eriksson, R. Karlsson, M.R. Yahya, Rolling resistance model, fuel consumption model and the traffic energy saving potential from changed road surface conditions. Statens väg-och transportforskningsinstitut. http://urn.kb.se/resolve?urn=urn:nbn:se:vti:diva-1830.
[118] J. Hooghwerff, E.W. van Gils, H.F. Reinink, Influence of road surface type on rolling resistance (2013).
[119] U. Sandberg, A. Bergiers, J.A. Ejsmont, L. Goubert, R. Karlsson, M. Zöller, Road surface influence on tyre/road rolling resistance. http://urn.kb.se/resolve?urn=urn:nbn:se:vti:diva-15699.
[120] J.R. Willis, M.M. Robbins, M. Thompson, Effects of pavement properties on vehicular rolling resistance: A literature review (2015).
[121] H.G. Kerali, J.B. Odoki, E.E. Stannard, Overview of HDM-4 (2000).
[122] B. Mashadi, S. Ebrahimi-Nejad, M. Abbaspour, A rolling resistance estimate using nonlinear finite element numerical analysis of a full three-dimensional tyre model, Proc. Inst. Mech. Eng., Part D: J. Automob. Eng. 233 (1) (2019) 147–160, https://doi.org/10.1177/0954407018802733.
[123] M. Yu, Z. You, G. Wu, L. Kong, C. Liu, J. Gao, Measurement and modeling of skid resistance of asphalt pavement: A review, Constr. Build. Mater. 260 (2020), 119878, https://doi.org/10.1016/j.conbuildmat.2020.119878.
[124] P. Farhadi, A. Golmohammadi, A.S. Malvajerdi, G. Shahgholi, Tire and soil effects on power loss: Measurement and comparison with finite element model results, J. Terramech. 92 (2020) 13–22, https://doi.org/10.1016/j.jterra.2020.09.004.
[125] B.S.S. Tchuigwa, J. Krmela, J. Pokorny, A literature review on tire component requirements, Perner's Contacts 16 (2) (2021), https://doi.org/10.46585/pc.2021.2.1740.
[126] X. Guo, Z. Zheng, M. Zang, S. Chen, A multi-sphere DE-FE method for traveling analysis of an off-road pneumatic tire on irregular gravel terrain, Eng. Anal. Bound. Elem. 139 (2022) 293–312, https://doi.org/10.1016/j.enganabound.2022.04.003.
[127] J. Marais, G. Venter, Numerical modelling of the temperature distribution in the cross-section of an earthmover tyre, App. Math. Model. 57 (2018) 360–375, https://doi.org/10.1016/j.apm.2018.01.018.
[128] P. Yang, M. Zang, H. Zeng, An efficient 3D DEM-FEM contact detection algorithm for tire-sand interaction, Powder Technol. 360 (2020) 1102–1116, https://doi.org/10.1016/j.powtec.2019.10.069.
[129] Z. El-Sayegh, M. Sharifi, F. Gheshlaghi, A. Mardani, Development of an HLFS agricultural tire model using FEA technique, SN Appl. Sci. 1 (11) (2019) 1454, https://doi.org/10.1007/s42452-019-1524-y.
[130] S.N. Ali, Rolling resistance estimation for PCR tyre design using the finite element method. In Finite Element Methods and Their Applications, IntechOpen (2020), https://doi.org/10.5772/intechopen.94144.
[131] W.A.A.S. Premarathna, J.A.S.C. Jayasinghe, P. Gamage, C.D. Senanayake, K. K. Wijesundara, R.R.M.S.K. Ranatunga, Analysis of factors influencing on performance of solid tires: Combined approach of design of experiments and thermo-mechanical numerical simulation, Eur. J. Mech. A. Solids 96 (2022), 104680, https://doi.org/10.1016/j.euromechsol.2022.104680.
[132] T.F. Fwa, Skid resistance determination for pavement management and wet-weather road safety, Int. J. Transp. Sci. Technol. 6 (3) (2017) 217–227, https://doi.org/10.1016/j.ijtst.2017.08.001.
[133] R.B. Kogbara, E.A. Masad, E. Kassem, A. Scarpas, A state-of-the-art review of parameters influencing measurement and modeling of skid resistance of asphalt pavements, Constr. Build. Mater. 114 (2016) 602–617, https://doi.org/10.1016/j.conbuildmat.2016.04.002.
[134] H. Zhang, K. Anupam, A. Scarpas, C. Kasbergen, Comparison of different micromechanical models for predicting the effective properties of open graded mixes, Transp. Res. Rec. 2672 (28) (2018) 404–415, https://doi.org/10.1177/0361198118794713.
[135] H. Zhang, K. Anupam, T. Scarpas, C. Kasbergen, S. Erkens, L. Al Khateeb, Continuum-based micromechanical models for asphalt materials: Current practices & beyond, Constr. Build. Mater. 260 (2020), 119675, https://doi.org/10.1016/j.conbuildmat.2020.119675.
[136] P. Liu, D. Wang, F. Otto, J. Hu, M. Oeser, Application of semi-analytical finite element method to evaluate asphalt pavement bearing capacity, Int. J. Pavement Eng. 19 (6) (2018) 479–488, https://doi.org/10.1080/10298436.2016.1175562.
[137] Z. Sun, C. Kasbergen, A. Skarpas, K.N. van Dalen, K. Anupam, S.M.J.G. Erkens, A nonlinear spectral element model for the simulation of traffic speed deflectometer tests of asphalt pavements, Int. J. Pavement Eng. 23 (4) (2022) 1186–1197, https://doi.org/10.1080/10298436.2020.1795170.
[138] C. Wu, H. Wang, J. Zhao, X. Jiang, Q. Yanjun, B. Yusupov, Prediction of viscoelastic pavement responses under moving load and nonuniform tire contact stresses using 2.5-D finite element method, Math. Probl. Eng. 2020 (2020) 1–16, https://doi.org/10.1155/2020/1029089.
[139] E.S.K. Mensahn, S.A. Wada, L. Lugeiyamu, Roadway pavement design methods, structural approaches and relevant computer algorithms: A critical review, Int. J. Trans. Eng. Technol. 8 (1) (2022), https://doi.org/10.11648/j.ijtet.20220801.12.
[140] H. Zhang, Q. Zhao, C. Peng, Response characteristics analysis and fatigue life assessment of asphalt pavement around the manhole, Shock Vib. 2020 (2020) 1–19, https://doi.org/10.1155/2020/8818543.
[141] Z. Shida, M. Koishi, T. Kogure, K. Kabe, A rolling resistance simulation of tires using static finite element analysis, Tire Sci. Technol. 27 (1999) 84–105, https://doi.org/10.2346/1.2135980.
[142] J.R. Luchini, J.M. Peters, R.H. Arthur, Tire rolling loss computation with the finite element method, Tire Sci. Technol. 22 (4) (1994) 206–222, https://doi.org/10.2346/1.2139542.
[143] W.V. Mars, J.R. Luchini, An analytical model for the transient rolling resistance behavior of tires, Tire Sci. Technol. 27 (3) (1999) 161–175, https://doi.org/10.2346/1.2135982.
[144] T. Lu, N.H. Thom, T. Parry, Numerical simulation of the influence of pavement stiffness on energy dissipation, Proceedings of the 13th International Conference on Computing in Civil and Building Engineering 30 (2010) 483–488.
[145] S. Pouget, C. Sauzéat, H.D. Benedetto, F. Olard, Viscous energy dissipation in asphalt pavement structures and implication for vehicle fuel consumption, J. Mater. Civ. Eng. 24 (5) (2012) 568–576, https://doi.org/10.1061/(ASCE)MT.1943-5533.0000414.
[146] G. Bazi, E.Y. Hajj, A. Ulloa-Calderon, P. Ullidtz, Finite element modelling of the rolling resistance due to pavement deformation, Int. J. Pavement Eng. 21 (3) (2020) 365–375, https://doi.org/10.1080/10298436.2018.1480778.
[147] S. Rajaei, K. Chatti, Mechanistic modeling of macro-texture's effect on rolling resistance. Advances in Materials and Pavement Performance Prediction II, CRC Press, 2020.
[148] Michelin, The tyre - Rolling resistance and fuel savings. Société de Technologie Michelin 23, rue Breschet, 63000 Clermont-Ferrand, 2003.
[149] N.J. Santero, A. Horvath, Global warming potential of pavements, Environ. Res. Lett. 4 (3) (2009), 034011, https://doi.org/10.1088/1748-9326/4/3/034011.
[150] L. Trupia, T. Parry, L.C. Neves, D. Lo Presti, Rolling resistance contribution to a road pavement life cycle carbon footprint analysis, Int. J. Life Cycle Assess. 22 (6) (2017) 972–985, https://doi.org/10.1007/s11367-016-1203-9.
[151] T. Wang, I.-S. Lee, A. Kendall, J. Harvey, E.-B. Lee, C. Kim, Life cycle energy consumption and GHG emission from pavement rehabilitation with different rolling resistance, J. Clean. Prod. 33 (2012) 86–96, https://doi.org/10.1016/j.jclepro.2012.05.001.
[152] T. Wang, J. Harvey, A. Kendall, Reducing greenhouse gas emissions through strategic management of highway pavement roughness, Environ. Res. Lett. 9 (3) (2014), 034007, https://doi.org/10.1088/1748-9326/9/3/034007.
[153] EPA's Office of Transportation and Air Quality (OTAQ), User guide for MOVES2014 (2014).
[154] International Carbon Bank & Exchange (ICBE), TCO_2 in gaseous volume and quantity of fuel type. https://www.icbe.com/carbondatabase/volumeconverter.asp.